

Grain core study of $\text{Fe}_{1-x}\text{Cr}_x$ nanograins obtained by mechanical alloying

This article has been downloaded from IOPscience. Please scroll down to see the full text article.

1999 J. Phys.: Condens. Matter 11 8341

(<http://iopscience.iop.org/0953-8984/11/42/314>)

View [the table of contents for this issue](#), or go to the [journal homepage](#) for more

Download details:

IP Address: 171.66.16.214

The article was downloaded on 15/05/2010 at 13:33

Please note that [terms and conditions apply](#).

Grain core study of $\text{Fe}_{1-x}\text{Cr}_x$ nanograins obtained by mechanical alloying

C Lemoine, A Fnidiki, D Lemarchand and J Teillet

Groupe de Métallurgie Physique UMR CNRS 6634, 76821 Mont-Saint-Aignan Cédex, France

Received 11 May 1999

Abstract. Mechanical alloying (MA) of $\text{Fe}_{1-x}\text{Cr}_x$ powder mixtures was performed over a wide range of concentration. Both x-ray diffraction and TEM analyses show that, after 30 hours of milling, the powder particles consist of nanocrystalline grains less than 10 nm in size. The kinetics of mixing is studied by Mössbauer spectrometry. This is the first time that the FeCr mixing state has been studied as a function of the milling conditions and the initial powder composition. This mixing state is defined by a parameter (d) calculated from the hyperfine field values.

The alloying process is weakly composition dependent (for $x \leq 40$ at.% Cr), but is linked to the energy input to the powder. Especially an energy threshold must be transferred to the powder to reach a complete alloying.

By studying the hyperfine field distributions of the Mössbauer spectra (for Cr < 40 at.%), it seems that the $\text{Fe}_{1-x}\text{Cr}_x$ nanograin cores are quite homogeneous in composition and have hyperfine parameters close to those of the bulk alloys.

1. Introduction

MA leads to an interdispersion of elements occurring through the repeated cold welding and fracture of free powder particles [1]. Since the 1970s a wide variety of equilibrium and metastable phases have been formed by MA of elemental powders. Recent progress in the understanding of the phase formation induced by MA is described in general publications [2–5].

During MA from an elemental powder mixture, the grain size decreases due to the mechanical deformation and reaches a nanometre scale [6]. At the same time, the elements mix together, their respective solubilities being enhanced by defects such as dislocations created by MA [7]. Progressively, the concentration gradients disappear and eventually the elements are mixed at the atomic scale. In fact, the MA process is more complex than this and the end product depends on many parameters such as the milling conditions [8–13] and the thermodynamic properties of the milled system.

At high temperature, the FeCr alloys are solid solutions, but during thermal treatment in the temperature range 44–830 °C, and near the equiatomic composition, an intermetallic phase σ can be formed. This phase is known to transform into bcc solid solution during ball milling [14]. Moreover, the FeCr binary system is quite interesting because the thermodynamic phase diagram shows a broad miscibility gap for a wide range of concentrations, the temperature at the top of the gap being about 800 °C [15]. These alloys are known to decompose (via nucleation and growth or spinodal decomposition) into Fe-enriched and Cr-enriched solid solution during thermal treatment between 400 and 500 °C [16–19]. Below this temperature range, the diffusion is too low to allow the

decomposition. The MA is performed at room temperature, but due to the plastic deformations, a temperature increase is expected. A controversy still exists concerning the temperature range of this increase [20–22]. Nevertheless, the temperature increase can be high enough to provoke thermally activated transformations. It is thus interesting to know whether a homogeneous $\text{Fe}_{1-x}\text{Cr}_x$ alloy can be produced by MA although Cr and Fe atoms ‘dislike’ each other.

The powder structure obtained by MA is quite specific, with particles of several micrometres consisting of nanocrystalline grains. When the grain size is small enough, the grain boundary fraction cannot be neglected. The study of the grain boundary and core grain structure is difficult because it requires accurate atomic level techniques. Mössbauer spectrometry is appropriate to study the specific problems of nanometre range [23]. In the case of FeCr powder mixture, Mössbauer spectrometry can be used because the hyperfine parameters (i.e. the isomer shift IS, the hyperfine field B_{hf}) are sensitive to a change of the ^{57}Fe nearest neighbour environment.

This work presents experimental results for the MA of an $\text{Fe}_{1-x}\text{Cr}_x$ powder mixture over a large range of concentrations. The discussion is essentially focused on the properties of magnetic grains in order to clarify the core properties of the nanocrystalline grains obtained by MA. All the results are useful for the understanding of the mechanical alloying kinetics of a binary system having a miscibility gap.

2. Experiment

MA of a mixture of pure Cr powder (99.0%) and pure Fe powder (99.9%) was carried out in a Fritsch planetary mill (‘Pulverisette P5’), using hardened steel vials and five balls (diameter = 20 mm). The weight of the mixed powder sample for each composition was about 12 g and the ball to powder weight ratio was 13:1. To minimize oxidation the loaded vials were always sealed under argon atmosphere. The powder composition varied from 0 to 90 at.% Cr. EDX analyses after 30 hours of milling indicate a metallic impurity level less than 3 at.% of iron. The milled powders were analysed by x-ray diffraction (XRD), and Mössbauer spectrometry.

X-ray diffraction measurements carried out on a Siemens powder diffractometer using $\text{Co K}\alpha$ radiation ($\lambda = 0.1789$ nm) allowed the average grain size (i.e. the size of the diffraction coherent domains) to be estimated. First, single line analysis using the Voigt function was used because few diffraction peaks are obtained [24]. This method was successful in determining the particle size of pure iron, but did not give satisfactory results when dealing with FeCr alloys because the lattice parameters of Fe ($a_{Fe} = 0.28664$ nm) and Cr ($a_{Cr} = 0.2884$ nm) are so close that diffraction peaks overlap. Thus, the well known Scherrer method was the only suitable method for the study. This method is not very accurate because it gives the domain size $D = 0.9\lambda / (\text{FWHM} \cdot \cos \theta)$ (FWHM = full width at half maximum intensity) neglecting the influence of strains. To confirm the x-ray diffraction results, transmission electron microscopy (TEM) analyses were performed. For these analyses, the powders were mortar attacked and then suspended in ethanol and scattered for a few minutes in an ultrasonic sound bath before being collected on a carbon/forvar grid.

Mössbauer spectra were recorded in transmission at room temperature using a ^{57}Co source in a rhodium matrix. The Mössbauer spectra were fitted with a least-squares technique using the histogram method related to a discrete distribution. The isomer shift (IS) at the ^{57}Fe nuclei is given relative to α -Fe at room temperature. A correlation between the hyperfine field (B_{hf}) and the IS is used to take into account the environment distributions.

3. Experimental results

3.1. Structure of the FeCr powder mixture

The grain size can be inferred from x-ray diffraction using the Scherrer method, but not chemical information such as the fraction of Cr mixed with Fe because the diffraction peaks of Cr and Fe overlap.

The diffraction patterns of the $Fe_{60}Cr_{40}$ alloys show broadened diffraction peaks and a decrease of peak intensity with milling time (figure 1(a)). This is attributed to the refinement

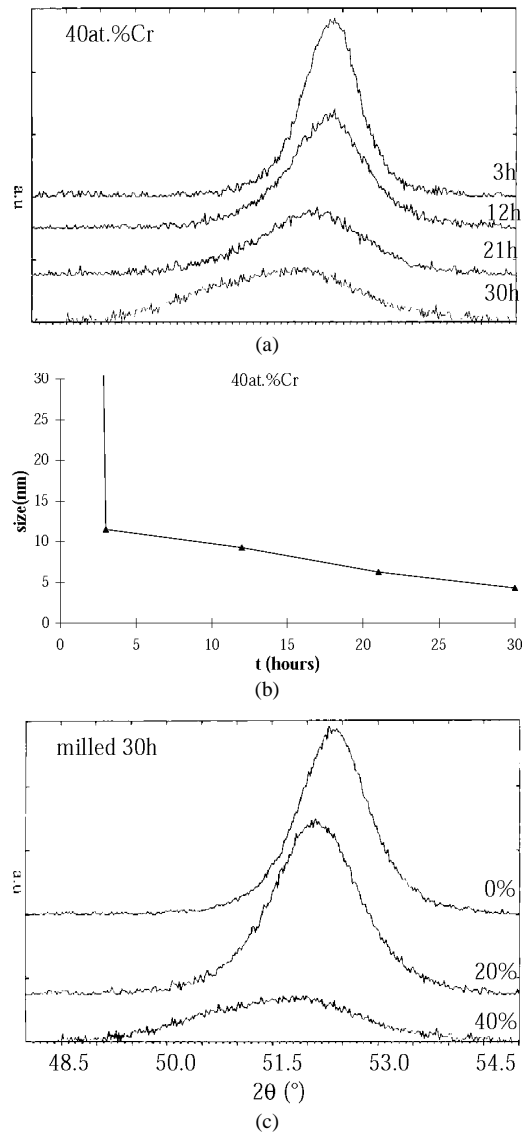


Figure 1. (a) X-ray diffraction patterns of an $Fe_{60}Cr_{40}$ powder mixture after different milling times; (b) the grain size versus the milling time; (c) x-ray diffraction patterns of powders with different Cr content, milled 30 h.

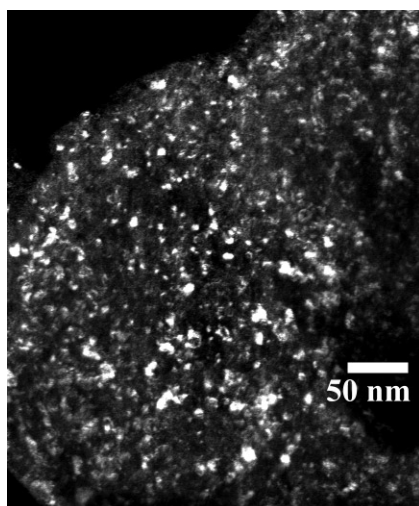


Figure 2. Dark field image with a portion of the (110) FeCr ring, of an Fe₆₀Cr₄₀ particle obtained after 12 hours of milling.

of the crystallite size and the increase in internal strain [25]. The crystallite size (figure 1(b)) decreases as the milling time increases and tends to reach about 5 nm after 30 hours of milling. At this stage, the peak is very broad and no longer symmetric probably due to a decrease of the crystallinity.

These results are in good agreement with TEM results (figure 2) where the dark field image shows crystallites (in white) of about 4 nm.

Despite the lack of accurate size measurements, x-ray diffraction and TEM analyses prove that mechanical alloying of a mixture of FeCr leads to nanocrystalline grains measuring less than 10 nm.

3.2. Mössbauer spectrometry results

Mössbauer spectra at RT of Fe_{1-x}Cr_x with $x = 20, 40, 90$ at.% Cr after different milling times are reported in figure 3. For $x = 20$ at.%, the hyperfine field at the ⁵⁷Fe nucleus (B_{hf}) decreases with the milling time due to the milling of the chromium atoms with Fe atoms. At the same time, the peak width of the sextuplets increases due to the different B_{hf} corresponding to different ⁵⁷Fe environments. The hyperfine field distributions (HFDs) show this tendency. After 3 h of milling the HFD shows a narrow peak centred on 33 T which is characteristic of the Fe not yet alloyed with Cr. With an increased milling time, this peak widens until a Gaussian type distribution shape is reached, characteristic of the bulk FeCr solid solution (Fe and Cr atoms are randomly distributed on the bcc lattice).

For $x = 90$ at.% (figure 3(c)), after 12 h of milling, the Mössbauer spectra consist only of a paramagnetic contribution, as expected from the magnetic diagram of the bulk Fe₁₀Cr₉₀ [26]. Nevertheless, if the spectra are recorded between -2 and $+2$ mm s⁻¹ to improve the accuracy, the paramagnetic peak appears much broader due to different contributions. By fitting with an HFD, two main contributions appear: one is centred on 0.5 T and the other on 2.5 T. The high field component can be attributed to the grain boundaries and the other to the crystalline grains [27].

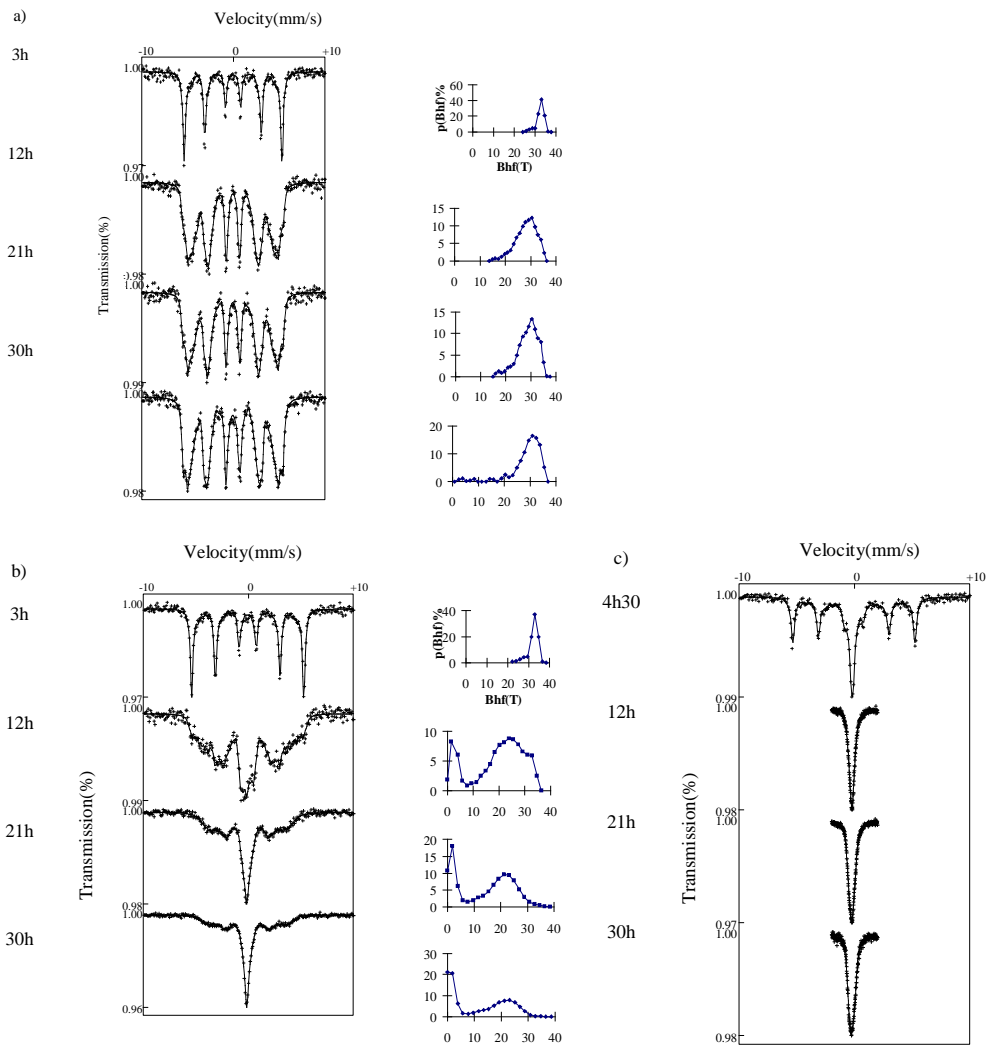


Figure 3. Mössbauer spectra and the corresponding HFDs of (a) $Fe_{80}Cr_{20}$ and (b) $Fe_{60}Cr_{40}$ powder mixture; (c) Mössbauer spectra of an $Fe_{10}Cr_{90}$ powder mixture.

For $x = 40$ at.% (figure 3(b)), the Mössbauer spectra are comprised of both a paramagnetic and a magnetic contribution. The magnetic contribution is attributed to the $Fe_{60}Cr_{40}$ solid solution as expected from the magnetic diagram [26]. The paramagnetic contribution is probably due to the grain boundaries disordered by gas contamination (nitrogen and oxygen). Indeed it has been observed by Ogino *et al* [28] that mechanical alloying of FeCr powder in nitrogen gas gives a paramagnetic contribution to the Mössbauer spectra. This contribution has been attributed to the grain boundaries which are nitrogen enriched. Nevertheless, further studies must be done to clarify this point, and all the results will be published in a forthcoming publication.

Hence, in the following study, only the magnetic contributions are considered. These contributions are attributed to the core of the nanocrystalline grains. In order to compare

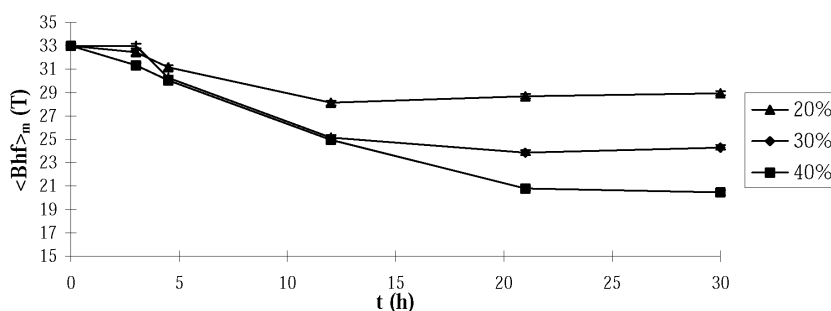


Figure 4. $\langle B_{hf} \rangle_m$ of the magnetic contributions of the HFDs versus the milling time for different Cr contents.

the hyperfine parameters of the nanocrystalline powders with those of the bulk alloy, the mean hyperfine fields are calculated considering the magnetic contribution of the HFD only: $\langle B_{hf} \rangle_m = (\sum_i p_i B_i) (\sum_i p_i)^{-1}$. $\langle B_{hf} \rangle_m$ decreases with the milling time during the first hours of milling (figure 4) and levels off after 21 h of milling time. The decrease of $\langle B_{hf} \rangle_m$ is due to the progressive mixing of Cr with Fe as the Cr is known to decrease $\langle B_{hf} \rangle_m$ at the ^{57}Fe nucleus. The plateau corresponds to a complete mixing between Cr and Fe. This state is called the 'stationary mixing state'.

4. Discussion

4.1. Kinetics of the mechanical alloying

To study the MA kinetics a mixing parameter d is defined as follows: $d = (33 - \langle B_{hf} \rangle_m) / (33 - \langle B_{hf} \rangle_{mst})$, where 33 T is the hyperfine field of the unmixed Fe, $\langle B_{hf} \rangle_{mst}$ is the mean hyperfine field of the distribution at the stationary mixing state (in tesla) and $\langle B_{hf} \rangle_m$ is the mean hyperfine field of the magnetic contribution. This parameter represents the mixing state: it varies from 0 (unmixed) to 1 (completely mixed) and it is necessary to know $\langle B_{hf} \rangle_{mst}$. For this reason, $\langle B_{hf} \rangle_{mst}$ of different mixtures was determined at 30 h of milling (at the assumed stationary mixing state). $\langle B_{hf} \rangle_m$ versus x is represented in figure 5 and is compared with magnetic bulk $\text{Fe}_{1-x}\text{Cr}_x$ results [29]. This indicates that the nanocrystalline grains of FeCr at the stationary mixing state have, on average, a magnetic behaviour very close to the bulk alloys.

From $\langle B_{hf} \rangle_m$ of HFD and figure 5, the amount of chromium which mixes with the Fe as a function of the milling time is deduced. The profile obtained (figure 6) can be explained by the simultaneous effect of deformation and intermixing during MA [30]. During the first hours of milling, a layered structure is formed [1] with alternate Cr and Fe layers. During the milling process, the plastic deformations accelerate atoms diffusion at the interface and reduce the difference in composition across the interface. Moreover, atomic transport from the interface to the interior of the layer takes place by diffusion (which is enhanced by the diffusion of solutes along the dislocation cores [7]). The mixing process continues until no concentration gradient exists, i.e. the Fe and Cr powders are completely alloyed ($d = 1$).

Moreover, as the kinetics of intermixing depends on the mechanical deformation, it thus depends on the milling conditions which can be studied in terms of energy transfer to the powder. The collision model of Burgio *et al* [9] was used to calculate the energy supplied to the powder during the MA process. This model supposes that the energy is transferred only by collisions between balls and vial walls. Iassonna *et al* [12] have shown that this assumption agreed well with experimental results. The power P transferred from the mill to the system

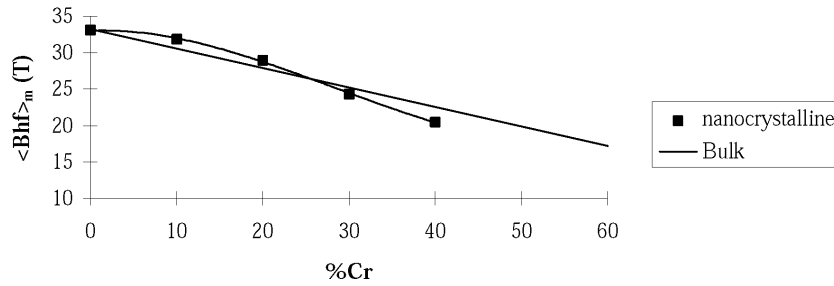


Figure 5. $\langle B_{hf} \rangle_m$ of the magnetic contributions of the experimental HFDs versus the Cr content after 30 hours of milling. The ‘bulk’ corresponds to the results obtained by Johnson *et al* for bulk FeCr alloys [29].

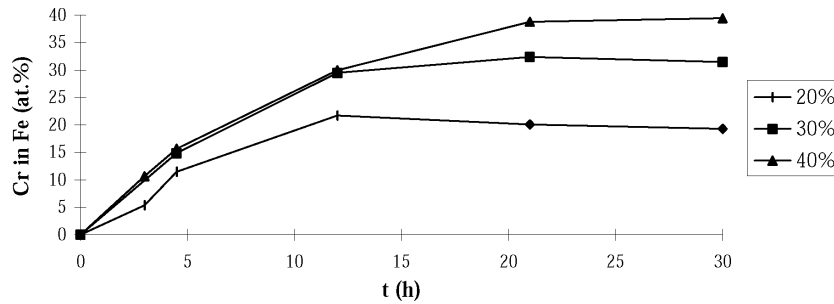


Figure 6. The Cr content mixed with the Fe as a function of the milling time.

during collisions is expressed as follows:

$$P = \phi_b \Delta E_b N_b f_b$$

where

- ΔE_b is the total energy released by the ball during the series of collision events: it depends on the geometry of the milling tools (ball and vial diameter, plate diameter, volume of the vial) and on the rotation speed of the vial and the plate.
- f_b is the frequency with which the balls are launched. This frequency is considered to be proportional to the relative speed of rotation of the mill.
- N_b is the number of balls (five in our case)
- ϕ_b is an empirical factor able to account for the degree of filling of the vial. In our case, this parameter is almost equal to 1.

In our study, the only parameter that has been varied is the rotation speed; the other parameters have been set constant to have an optimum degree of filling ϕ_b . For a given rotation speed the power transferred is the same whatever the milling time. But it is clear that the milling time must also be considered for the MA alloying process. So, it is better to consider the integral energy transferred to the powder during the mechanical process [9]: $W = Pt$ /powder weight, t being the milling time. The W unit is the watt hour per gram. The mixing parameter d is represented versus W (figure 7). A threshold value of W seems to be required for a complete mixing, and it is weakly dependent on the chromium content (for $x \leq 40\%$). Moreover, the alloying process seems to start only when a certain amount of energy is transferred to the powder. This is in good agreement with the incubation time for intermixing that Fultz *et al* have reported during MA of FeV [31]. Although the quantitative values are only very roughly estimated, the W calculation enables us to compare experimental results using different

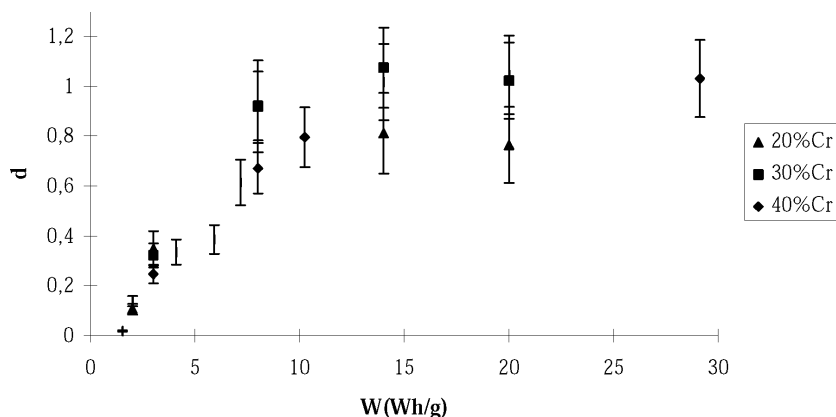


Figure 7. The mixing parameter d versus the integrated energy transferred to the powder W (calculated with the collision model of Burgio *et al* [9]).

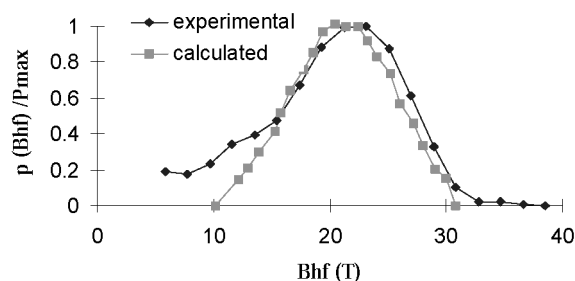


Figure 8. The experimental and calculated (from Dubiel's results on bulk FeCr alloys [32]) HFDs for $x = 40$ at.% Cr. P_{max} is the maximum probability of B_{hf} , used to normalize the HFD.

milling conditions. On the other hand, the knowledge of the milling parameters allows the time required to obtain a desired mixing state to be determined.

4.2. The characteristics of the stationary mixing state

As previously mentioned, $\langle B_{hf} \rangle_m$ remains constant after 30 hours of milling. The state reached is called a 'stationary mixing state'. $\langle B_{hf} \rangle_m$ values at the stationary state are very close to that of bulk alloys; nevertheless, this is not sufficient to draw conclusions about the similarity between the two states. Indeed, it is obvious that two alloys with different HFD can have the same $\langle B_{hf} \rangle_m$. Hence, it seems useful to study the HFD of the mechanically alloyed FeCr powders and compare it to that of the bulk alloys.

The bulk crystalline $\text{Fe}_{1-x}\text{Cr}_x$ alloys have been widely studied by Mössbauer spectrometry. The hyperfine field is usually studied assuming the additive relation: $B_{hf}(m, n) = B(0, 0) + m\Delta B_1 + n\Delta B_2$, where $B_{hf}(m, n)$ stands for the hyperfine field at the Fe nuclei having m Cr in the first co-ordination sphere, and n Cr in the second one. ΔB_1 and ΔB_2 are the decrease of the B_{hf} obtained by replacing an Fe atom with a Cr in the first and the second co-ordination shells respectively. The probability of obtaining $B_{hf}(m, n)$, in a randomly disordered FeCr solid solution, is assumed to be given by a binomial law: $C_8^m C_6^n (1-x)^{14-(m+n)} x^{m+n}$, x being the chromium content. The bulk alloy HFDs are calculated using ΔB_1 , ΔB_2 results of Dubiel *et al* [32].

Figure 8 shows that the experimental HFDs of the nanocrystalline Fe_{1-x}Cr_x powder obtained by MA are well fitted by the HFD of the bulk Fe_{1-x}Cr_x of the same concentration.

This proves not only that the magnetic nanocrystalline grains have the composition of the starting powder mixture, but also that they have a magnetic behaviour similar to that of the bulk alloys with the same composition. Although the grain size is very small, about 10 nm, no superparamagnetism is detected, so the results can be explained by a collective behaviour of the nanograins. However, further magnetic measurements are required to confirm this point. Moreover, the experimental HFDs being well fitted with a binomial distribution, it is possible to conclude that the alloy is homogeneous in composition after 30 hours of milling.

5. Conclusion

The MA of Fe_{1-x}Cr_x powder mixtures leads to nanocrystalline alloys with grain sizes of about 10 nm. After 30 hours of milling, a stationary mixing state is obtained and the powder is no longer a mixture of pure Fe and Cr but a true alloy. This alloy is obtained at the Mössbauer analysis scale i.e., at the atomic scale. A mixing state parameter (*d*) is defined to follow the kinetics of the mixing. The integrated energy transfers to the powder must reach a threshold to complete alloying, which is only weakly concentration dependent for $x \leq 40$ at.% Cr.

The study of the hyperfine field distributions shows that the nanocrystalline grains have (for $x < 40$ at.%) a magnetic behaviour similar to that of the bulk alloys.

Further studies will be performed to explain the paramagnetic contribution of the grain boundaries for $x = 40$ at.% Cr, and especially the contamination gas effect.

References

- [1] Benjamin J S and Volin T E 1974 *Metall. Trans.* **5** 1929
- [2] Suryanarayana C 1995 *Bibliography on Mechanical Alloying and Milling* (Cambridge: Cambridge International Science)
- [3] Ma E and Atzmon M 1995 *Materials Chem. Phys.* **39** 249
- [4] Koch C C 1991 *Materials Science and Technology: a Comprehensive Treatment* vol 15, ed R W Cahn (New York: VCH) p 195
- [5] Le Caer G 1997 *Ann. Chim.* **22** 341
- [6] Fecht H J 1992 *Nanostruct. Mater.* **1** 125
- [7] Schwarz R B 1998 *Mater. Sci. Forum* **269–272** 665
- [8] Abdelaoui M and Gaffet E 1995 *Acta Metall. Mater.* **43** 1087
- [9] Burgio N, Iassona A, Magini M, Martelli S and Padella F 1991 *Nuovo Cimento* **13** 459
- [10] Delogu F, Monagheddu M, Mulas G, Schiffini L and Cocco G 1998 *J. Non Cryst. Solids* **232** 383
- [11] Schiffini L and Cocco G 1998 *J. Non Cryst. Solids* **239** 383
- [12] Iassona A and Magini M 1996 *Acta Mater.* **44** 1109
- [13] Chen Y, Le Hazif R and Martin G 1992 *Solid State Phenom.* **23** 271
- [14] Yang H, Di L M and Bakker H *Intermetallics* **1** 29
- [15] Kubaschewski O 1922 *Iron-Binary Phase Diagrams* (Berlin: Springer) p 32
- [16] Chandra D and Schwartz L H 1971 *Metall. Trans.* **2** 511
- [17] De Nys T and Gielen P M 1971 *Metall. Trans.* **2** 1423
- [18] Kuwano H 1985 *Trans. Jap. Inst. Met.* **26** 473
- [19] Dubiel S M and Inder G 1987 *Z. Metallkd.* **78** 544
- [20] Schwarz R B and Koch C C 1986 *Appl. Phys. Lett.* **49** 146
- [21] Bhattacharya A K and Arzt E 1992 *Scr. Metall. Mater.* **27** 749
- [22] Ecker J 1988 *J. Appl. Phys.* **64** 3224
- [23] Le Caer G and Delcroix 1996 *Nanostruct. Mater.* **7** 127
- [24] Keijser T H H, Langford J J, Mittermeijer E J and Vogels A B P 1982 *J. Appl. Phys.* **15** 308
- [25] Hellstern E, Fecht H J, Fu Z and Johnson W L 1989 *J. Appl. Phys.* **65** 305
- [26] Burke S K, Cywinski R, Davis J R and Rainford B D 1983 *J. Phys. F: Met. Phys.* **13** 451

- [27] Fultz B, Kuwano H and Ouyang H 1995 *J. Appl. Phys.* **77** 3458
- [28] Ogino Y, Namba K and Yamasaki T 1993 *ISIJ Int.* **33** 420
- [29] Johnson C E, Ridout M S and Cranshaw T E 1963 *Proc. Phys. Soc.* **81** 1079
- [30] Pabi S K, Das D, Mahapatra T K and Manna I 1998 *Acta Mater.* **46** 3501
- [31] Fultz B, Le Caër G and Matteazzi P 1989 *J. Mater. Res.* **4** 1450
- [32] Dubiel S M and Zukrowski J 1981 *J. Magn. Magn. Mater.* **23** 214